in shifts from the trans 1:2 and the trans 1:1 complexes can be explained by a geometric distortion of the 1:1 complex which has a pyridine molecule at one axial position and a solvent molecule at the other axial position. This type of distortion would change both the geometric terms and the magnetic anisotropy of this complex. The slope of the line (Figure 6) of the trans 1:1 complex is positive while the slopes of the lines from all of the other complexes are negative. The positive slope of this line shows that the contribution of the dipolar interaction to the total shift is positive and the negative shift which is observed is due to the large negative intercept. The positive dipolar shift shows either that the magnetic anisotropy has changed sign (χ_x or $\chi_y > \chi_z$) or that $G(\theta,r)$ has a negative value. This angular term has negative values when $\theta > 54.4°$ and less than 125.6°. A relatively large distortion in the relative geometry of this complex would be required to produce either a change in the sign of the magnetic anisotropy or a large value of θ.

Conclusions

Our variable-temperature ^{19}F NMR investigation of pyridine complexes of $Co(HFAA)_2$ clearly demonstrates that cis and trans isomers of both 1:1 and 1:2 complexes are formed in acetone solutions. The cis isomer is favored over the trans isomer in both the 1:1 and 1:2 complexes. At higher temperatures interconversion of the isomers rapidly averages the dipolar contribution to the shifts and an exchange narrowed line with a shift dominated by the Fermi contact interaction is observed. The pyridine complex of $Ni(HFAA)_2$ exhibits a single ^{19}F NMR line over the accessible temperature range. The anisotropy of the magnetic susceptibility of nickel complexes is small and the shift which is observed is mainly due to the Fermi contact interaction. If cis and trans isomer are formed by $Ni(HFAA)_2(py)_2$, the dipolar shifts are not large enough to allow one to observe individual NMR lines from different species. At lower temperatures interconversion of the various cobalt complexes is slow and large dipolar shifts are observed from the various species. The shifts which are observed can be accounted for by differences in the relative geometry of the trifluoromethyl groups in the complexes. The components of the magnetic susceptibility may also vary in complexes with different structures. Data from earlier studies of $Co(AA)_2(py)_2$ have been analyzed by assuming that only the trans isomer is present in solution. If the protonated AA behaves in the same manner as the fluorinated analogue, the NMR spectra which are observed at room temperature are due to a rapidly averaged mixture of cis and trans isomers and the interpretation of the relative contributions of the Fermi contact and dipolar shifts needs to be reconsidered. Our study demonstrates that care must be taken not only in the separation of Fermi and dipolar shifts of paramagnetic metal complexes but also in determining the molecular species present in solution which can contribute to the total shift.

Acknowledgment. This work was supported in part by National Institutes of Health Grant GM-22793.

Registry No. $Co(HFAA)_2$, 19648-83-0; $Ni(HFAA)_2$, 14949-69-0; $Ni(HFAA)_2(py)_2$, 56586-65-3; *cis*-$Co(HFAA)_2(py)$, 77321-16-5; *trans*-$Co(HFAA)_2(py)$, 77398-31-3; *cis*-$Co(HFAA)_2(py)_2$, 58207-58-2; *trans*-$Co(HFAA)_2(py)_2$, 42866-33-1.

Contribution from the Department of Chemistry, University of Massachusetts, Amherst, Massachusetts 01003, and the Department of Physical Chemistry, University of Nijmegen, Toernooiveld, 6525 ED Nijmegen, The Netherlands

Crystal Structures of the Picoline *N*-Oxide Complexes $M(4\text{-}CH_3C_5H_4NO)_6(ClO_4)_2$ (M = Cu, Zn) and EPR Spectra of the Pure and Zinc-Doped Copper Complexes

J. S. WOOD,* R. O. DAY, C. P. KEIJZERS, E. DE BOER, A. E. YILDIRIM, and A. A. K. KLAASSEN

Received September 22, 1980

The hexakis(4-picoline *N*-oxide)copper and -zinc perchlorate complexes crystallize in the monoclinic system, space group $P2_1/c$, with the following unit cell dimensions: for the copper complex $a = 9.523$ (5) Å, $b = 10.707$ (8) Å, $c = 20.512$ (16) Å, and $\beta = 92.47$ (6)°; for the zinc complex, $a = 9.467$ (5) Å, $b = 10.760$ (5) Å, $c = 20.531$ (9) Å, and $\beta = 92.46$ (4)°. The structures were solved with the use of approximately 2400 independent reflections collected for each complex on a single-crystal diffractometer using Mo Kα radiation at ambient temperature. The final, conventional residuals were 0.097 and 0.082 for those reflections with $I > 2\sigma(I)$, these rather high values being the result of the limited sizes of the data sets available for the structure determinations. While the complex cations in the two salts have only $\bar{1}$ symmetry, the coordination polyhedron in the zinc complex comes close to octahedral geometry with an average Zn–O distance of 2.114 Å. The coordination geometry for the copper complex, however, is in accord with the presence of a static Jahn–Teller distortion, the Cu–O distances being 1.965, 2.008, and 2.385 Å. Single-crystal EPR measurements, at both X- and Q-band frequencies, are also indicative of tetragonally elongated geometries for the copper-containing cation, both in the pure complex and in the case when it is doped into the zinc complex. The principal values of the g tensor average 2.32, 2.12, and 2.07. In the pure complex, the cations are oriented in approximately a ferrodistortive arrangement, and there is no evidence from the EPR spectra for any appreciable magnetic exchange between the two nonequivalent sites in the monoclinic cell. For the doped system, there is no evidence for the operation of a dynamic Jahn–Teller effect even though the zinc host complex is approximately octahedral.

Introduction and Summary

The hexakis(pyridine *N*-oxide) complexes of copper(II) salts, $Cu(C_5H_5NO)_6X_2$ ($X = ClO_4^-$, BF_4^-, NO_3^-), exhibit dynamic and cooperative Jahn–Teller distortions and have been extensively investigated both by ourselves[1,2] and by other workers[3,4] using EPR and diffraction techniques. At very low temperatures, heat capacity measurements indicate that magnetic ordering occurs.[5] The planar antiferromagnetism observed for the fluoborate salt and the linear antiferromagnetism for the perchlorate salt are in accord respectively

* To whom correspondence should be addressed at the University of Massachusetts.

(1) Wood, J. S.; de Boer, E.; Keijzers, C. P. *Inorg. Chem.* **1979**, *18*, 904.
(2) Wood, J. S.; Keijzers, C. P.; de Boer, E.; Buttafava, A. *Inorg. Chem.* **1980**, *19*, 2213.
(3) Reinen, D.; Krause, S. *Solid State Commun.* **1979**, *29*, 691.
(4) O'Connor, C. J.; Sinn, E.; Carlin, R. L. *Inorg. Chem.* **1977**, *16*, 3314.
(5) Algra, H. A.; de Jongh, L. J.; Carlin, R. L. *Physica B+C (Amsterdam)* **1978**, *93*, 24.

0020-1669/81/1320-1982$01.25/0

with ferrodistortive and antiferrodistortive coupling of neighboring tetragonally elongated complexes.[6] For the nitrate salt, two crystalline modifications have been obtained:[2] a monoclinic form in which the complex cations are approximately ferrodistortively ordered at room temperature and a trigonal form (isostructural with the fluoborate and perchlorate salts[7]) which contains antiferrodistortively coupled complexes below the Jahn–Teller transition temperature.[2] The forms of the cooperative effects in these complexes are strongly influenced not only by the nature of the anion but also by the solvent used for preparation and crystal growing. Since the origins of these effects, in particular the role of the solvent, are not understood, we sought further examples of dynamic and cooperative Jahn–Teller effects in closely related copper(II) species. We elected to examine the 4-picoline *N*-oxide complex $Cu(4\text{-}CH_3C_5H_4NO)_6(ClO_4)_2$, the isolation of which has previously been reported.[8] In addition the analogous zinc complex was prepared in the hope that it would prove a suitable host for EPR studies. Our X-ray structural results, described herein, showed that the two complexes are isomorphous but that the coordination geometry of the zinc atom more closely approaches an octahedron than does that of copper. The packing arrangement in the copper complex is in fact very similar to that in the monoclinic modification of the pyridine *N*-oxide nitrate complex $Cu(C_5H_5NO)_6(NO_3)_2$.[9] The orientation of the cations in the unit cell may be described as being approximately ferrodistortive. The EPR spectra of single crystals exhibit for an arbitrary orientation, two lines from the two magnetically inequivalent sites in the unit cell, between which only very little magnetic exchange exists. This contrasts with the exchange narrowed EPR spectra of the trigonal (pyridine *N*-oxide)–Cu complexes. The EPR measurements indicate also that when doped into the zinc complex, the copper complex adopts its typically tetragonally elongated geometry, characteristic of a static Jahn–Teller effect, even at room and higher temperatures. In terms of the familiar warped Mexican hat potential surface arising from the $E \otimes e$ vibronic coupling scheme,[10] these measurements indicate that the surface is sufficiently distorted from C_{3v} symmetry such that only one well is significantly occupied at all temperatures. We had thought that with the near octahedral zinc complex as host lattice, the copper ion might exhibit a dynamic Jahn–Teller effect, with unequal but significant populations of the three wells. This situation occurs, for example, with the $Cu(H_2O)_6^{2+}$ ion in the monoclinic zinc Tutton's salt host crystal, and detailed study of the temperature dependence of the EPR has yielded important information on the nature of the reorientation process and the barrier heights between the three potential wells.[11]

Experimental Section

The hexacoordinated complexes $M(CH_3C_5H_4NO)_6(ClO_4)_2$ were prepared by reaction of excess 4-picoline *N*-oxide with copper and zinc perchlorates in methanolic solution.[8] Crystals suitable for X-ray and EPR studies were obtained from acetonitrile and dichloromethane solutions, and analyses of both copper and zinc complexes conformed satisfactorily to the above formulation. Preliminary photographic X-ray examination indicated that crystals of both complexes belonged to the monoclinic system, space group $P2_1/c$, the similarity in cell dimensions and zero level diffraction pattern suggesting isomorphism of the two structures.

1. Collection and Reduction of X-ray Data. Diffraction data were collected on an Enraf-Nonius CAD-4 diffractometer equipped with a graphite monochromator using Mo Kα radiation ($\lambda(K\alpha_1)$ = 0.709 30 Å, $\lambda(K\alpha_2)$ = 0.713 59 Å) and at a tube takeoff angle of 3.1°. The lattice constants were determined by least-squares refinements from the setting angles of 25 reflections in the region $20° < 2\theta < 27°$ and at a temperature of 24 °C. They are respectively a = 9.523 (5) Å, b = 10.707 (8) Å, c = 20.512 (16) Å, and β = 92.47 (6)° for the copper complex and a = 9.467 (5) Å, b = 10.760 (5) Å, c = 20.531 (9) Å, and β = 92.46 (4)° for the zinc complex. A unit cell content of two molecules gives a calculated density of 1.46 g cm^{-3} for both complexes, and the assignment Z = 2 was confirmed by successful solution of the structures. Intensity data for both complexes were collected with the use of the ω–2θ scan mode with a scan range of $(0.75 + 0.35 \tan \theta)°$ centered about the calculated Mo K α peak position. This scan range was extended an extra 25% on either side for measurement of the background radiation. The crystals used for data collection were sealed into capillaries and had dimensions 0.12 × 0.20 × 0.25 mm (Cu complex) and 0.10 × 0.35 × 0.35 mm (Zn complex). The scan rates varied from 0.75° to 4°/min, the rate used for each reflection having been determined from a prescan. The intensity I for each reflection was obtained from $I = F/S(P - 2(B_1 + B_2))$ where P and B_i are peak and background counts, S is an integer inversely proportional to the scan rate, and F is either unity or a multiplier to account for the occasional attenuation of the diffracted beam. The standard deviations in the intensities were computed as

$$\sigma(I) = [(F/S)^2[P + 4(B_1 + B_2)] + 0.002I^2]^{1/2}$$

A total of 2392 independent reflections for the zinc complex and 2385 reflections for the copper complex were measured in the range $2° \leq 2\theta_{Mo} \leq 44°$. Six standard reflections distributed widely in reciprocal space, and monitored after every 100 min of X-ray exposure time, gave no indication of crystal deterioration or loss of alignment. Sampling of the region $44° < 2\theta_{Mo} \leq 50°$ indicated that extremely few reflections having any significant intensity could be observed at higher diffraction angles than 44°. The rather limited extent of the resulting data sets for the two structures, with only ca. 65% of the reflections having $I > 2\sigma(I)$ and a consequent low reflection to parameter ratio, led, we believe, to the rather high final R values obtained at convergence, and to a lower level of accuracy for the final parameters than is normally desirable. No corrections were made for absorption ($\mu_{Mo\,K\alpha}$ is 8.1 cm^{-1} for the copper complex and 8.2 cm^{-1} for the zinc complex). Intensities were reduced to relative amplitudes by use of Lorentz and polarization corrections including corrections for the monochromator.

2. Solution and Refinement. In space group $P2_1/c$ the complex cations $M(CH_3C_5H_4NO)_6^{2+}$ are required to possess $\bar{1}$ symmetry. Initial coordinates for the nonhydrogen atoms of the three independent picoline *N*-oxide ligands of the zinc complex were obtained from the direct methods program MULTAN, and a difference electron density map, based on structure factors calculated from these atomic coordinates, yielded position parameters for the perchlorate group. It was evident from this map that although the ClO_4^- ion was not statically disordered, it was undergoing librational motions of very large amplitudes. Isotropic unit-weighted full-matrix least-squares refinement[12] gave a conventional residual R ($=\sum||F_o| - |F_c||/\sum|F_o|$) of 0.14 and a weighted residual R_w ($=[\sum w(|F_o| - |F_c|)^2/\sum w|F_o|^2]^{1/2}$) of 0.16 for those reflections with $I > 3\sigma(I)$. Anisotropic refinement with variable weights confirmed the large thermal motion of the perchlorate ion and led to convergence after four cycles, with R = 0.082 and R_w = 0.100 for the 1576 reflections having $I > 2\sigma(I)$, a total of 268 variables being refined in a block fashion. The final "goodness of fit" parameter was 2.31.

The final positional parameters and isotropic thermal parameters determined for the zinc complex were used as input for the least-

(6) The terms ferro- and antiferrodistortive refer to the two common ordering arrangements of distorted (elongated) octahedra found in copper (or other Jahn–Teller active) complexes having extended structures such as $KCuF_3$ (perovskite) and Ba_2CuWO_6 (elpasolite). They have, however, been extended in appropriate cases to cover discrete complexes also. The ferrodistortive arrangement is that in which all tetragonal axes of the distorted octahedra are parallel, while in the antiferrodistortive arrangement, in any one layer of the structure, the tetragonal axes of neighboring octahedra are mutually orthogonal. The arrangements correspond respectively to preferential population of one ($\phi = 0$) or of two ($\phi = 2\pi/3$ and $4\pi/3$) minima in the potential energy surface.[10] For further details, see: Reinen, D.; Friebel, C. *Struct. Bonding (Berlin)* **1979**, *37*, 1.

(7) Day, R. O.; Wood, J. S. *Cryst. Struct. Commun.*, in press.

(8) Herlocker, D. W. *J. Inorg. Nucl. Chem.* **1972**, *34*, 384.

(9) Day, R. O.; Wood, J. S., unpublished work.

(10) Ham, F. S. In "Electron Paramagnetic Resonance"; Geschwind, S., Ed.; Plenum Press: New York, 1972.

(11) Getz, D.; Silver, B. L. *J. Chem. Phys.* **1974**, *61*, 638.

(12) The function minimized was $\sum w(|F_o| - |F_c|)^2$, the weights w being calculated as $(2LpF_o/\sigma(I))^2$.

Table I. Atomic Positional Parameters for $M(CH_3C_5H_4NO)_6(ClO_4)_2$ (M = Cu, Zn) (Values × 10^4; Esd's in Parentheses)

	M = Cu			M = Zn		
atom	*x*	*y*	*z*	*x*	*y*	*z*
M	0	1/2	1/2	0	1/2	1/2
O(1)	387 (10)	3260 (8)	4763 (4)	387 (8)	3170 (6)	4755 (3)
O(2)	−267 (10)	5449 (8)	4053 (4)	−355 (8)	5403 (7)	3999 (3)
O(3)	−2454 (12)	4619 (9)	5080 (5)	−2229 (8)	4643 (7)	5117 (4)
N(1)	−135 (11)	2330 (9)	5104 (5)	−165 (10)	2253 (6)	5116 (4)
N(2)	291 (12)	4740 (9)	3611 (5)	227 (9)	4702 (7)	3564 (4)
N(3)	−3306 (12)	5331 (10)	4712 (6)	−3135 (9)	5339 (8)	4756 (4)
C(11)	672 (15)	1890 (13)	5597 (6)	572 (12)	1824 (11)	5635 (5)
C(12)	151 (17)	841 (14)	5941 (7)	18 (13)	839 (10)	5987 (6)
C(13)	−1168 (16)	350 (12)	5773 (7)	−1254 (13)	299 (10)	5796 (6)
C(14)	−1943 (18)	847 (13)	5240 (8)	−1971 (13)	741 (10)	5233 (6)
C(15)	−1420 (15)	1825 (12)	4921 (8)	−1403 (12)	1737 (10)	4880 (6)
C(16)	−1760 (19)	−796 (15)	6148 (9)	−1856 (16)	−795 (12)	6162 (7)
C(21)	−578 (16)	3982 (15)	3259 (7)	−591 (12)	3856 (11)	3232 (6)
C(22)	−37 (15)	3203 (15)	2784 (7)	32 (13)	3105 (12)	2759 (6)
C(23)	1384 (15)	3219 (13)	2673 (6)	1436 (12)	3193 (11)	2647 (5)
C(24)	2285 (17)	4006 (18)	3050 (8)	2235 (14)	4060 (13)	3001 (6)
C(25)	1660 (16)	4736 (15)	3510 (8)	1624 (13)	4812 (13)	3454 (6)
C(26)	2083 (17)	2331 (15)	2181 (7)	2197 (14)	2338 (13)	2162 (6)
C(31)	−3682 (17)	6457 (15)	4950 (8)	−3582 (12)	6443 (10)	4994 (6)
C(32)	−4573 (19)	7205 (16)	4565 (8)	−4514 (13)	7177 (11)	4619 (7)
C(33)	−5034 (15)	6858 (15)	3938 (8)	−4986 (12)	6772 (11)	3988 (6)
C(34)	−4592 (16)	5665 (15)	3727 (7)	−4534 (12)	5601 (12)	3782 (6)
C(35)	−3762 (16)	4895 (15)	4115 (7)	−3623 (12)	4893 (11)	4162 (6)
C(36)	−5996 (18)	7705 (18)	3479 (10)	−5958 (13)	7572 (13)	3574 (6)
Cl	−4029 (4)	1164 (4)	3445 (2)	−4018 (4)	1187 (4)	3413 (2)
O(4)	−4824 (14)	715 (15)	2938 (6)	−4832 (10)	671 (9)	2914 (4)
O(5)	−3930 (35)	412 (30)	3893 (15)	−4143 (20)	566 (22)	3954 (7)
O(6)	−2859 (21)	1761 (26)	3321 (9)	−2648 (13)	1381 (21)	3273 (7)
O(7)	−4699 (26)	1924 (34)	3786 (18)	−4540 (24)	2240 (17)	3589 (13)

squares treatment of the data for the copper complex. Anisotropic refinement with variable weights led to convergence with $R = 0.097$ and $R_w = 0.143$ for the 1700 reflections with $I > 2\sigma(I)$. The "goodness of fit" parameter had the rather high value of 3.15. As for the zinc complex, the ClO_4^- ion was observed to be undergoing very extensive librational motion. The magnitudes of the thermal parameters are in fact high for all atoms in both structures, and this presumably is a consequence of the somewhat lower than average number of reflections having a significant amount of observed intensity. In an attempt to improve the structure factor agreement for both copper and zinc complexes, the four ring hydrogen atoms of each ligand were included as fixed contributions in final cycles of refinement. These contributions did not lead to significant improvement in the weighted residuals or "goodness of fit" parameters however. The resulting conventional *R* values were 0.082 and 0.096 for the zinc and copper complexes, respectively.

All computations were carried out on a CDC Cyber-175 computer using LINEX, a modification of the Busing and Levy full-matrix least-squares program, ORFLS, Johnson's thermal ellipsoid plot program ORTEP, Zalkin's Fourier program FORDAP, and various locally written routines. Atomic scattering factors were taken from ref 13, and real and imaginary dispersion corrections for Cu and Cl were taken from the same source.[14]

The final positional parameters for the two complexes are listed in Table I while the anisotropic thermal parameters are deposited with the structure factor tables as part of the supplementary material.

3. EPR Measurements. Single-crystal measurements were carried out at both Q-band (35 GHz) and X-band (9.5 GHz) frequencies on a Varian E-12 spectrometer equipped with Oxford Instruments continuous-flow variable-temperature cryostats for low-temperature measurements and with a Varian high-temperature unit for sample temperatures above ambient. Magnetic fields were measured with a Bruker B-NM12 G meter and klystron frequencies with a Systron Donner (1037-S) and a Hewlett-Packard counter HP5246L. Single crystals studied at Q-band frequency at room temperature were mounted on a conventional X-ray goniometer, and measurements were made at 10° intervals for crystals rotating around the *a*, *b*, and *c* axes.

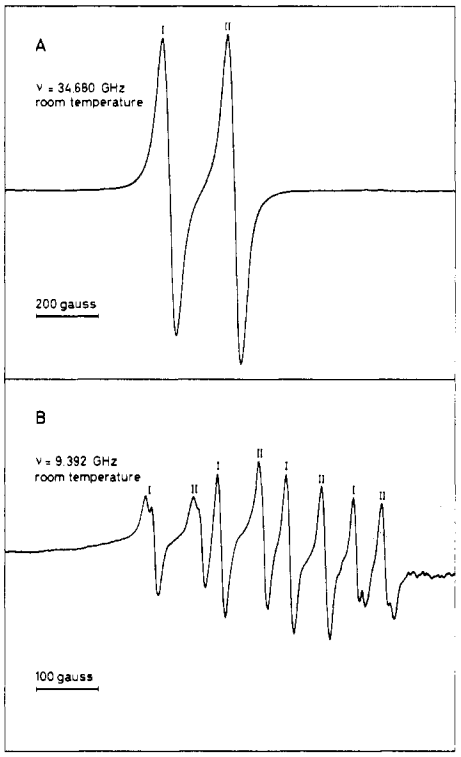

Figure 1. (A) Q-Band EPR spectrum of Cu(picoline *N*-oxide)$_6$(ClO$_4$)$_2$, showing the two magnetically inequivalent sites. The magnetic field is located in the a^*b plane, 20° from a^* and 70° from *b*. (B) X-Band EPR spectrum of 1% Cu/Zn(picoline *N*-oxide)$_6$(ClO$_4$)$_2$. The lines belonging to the two magnetically inequivalent sites are indicated. The magnetic field has the same orientation as in spectrum A.

The alignment was previously made by Weissenberg photography. In addition, a plane of arbitrary orientation was measured for the doped crystal, since the resolution of the spectra was rather poor in the (100) plane. For both doped and pure crystals, the two mag-

(13) "International Tables for X-ray Crystallography"; Kynoch Press: Birmingham, England, 1974; Vol. 4, pp 72–98.
(14) Reference 13, pp 149, 150.

Table II. Distances (Å) and Angles (Deg) in the Coordination Polyhedra of the $M(CH_3C_5H_4NO)_6(ClO_4)_2$ Complexes

	M = Cu	M = Zn
M-O(1)	1.965 (9)	2.068 (7)
M-O(2)	2.008 (9)	2.113 (7)
M-O(3)	2.385 (11)	2.160 (7)
O(1)-M-O(2)	90.3 (4)	89.0 (3)
O(1)-M-O(3)	92.8 (4)	92.4 (3)
O(2)-M-O(3)	91.4 (4)	91.7 (3)
M-O(1)-N(1)	120.2 (7)	119.0 (5)
M-O(2)-N(2)	119.4 (7)	119.5 (6)
M-O(3)-N(3)	116.1 (8)	116.5 (5)

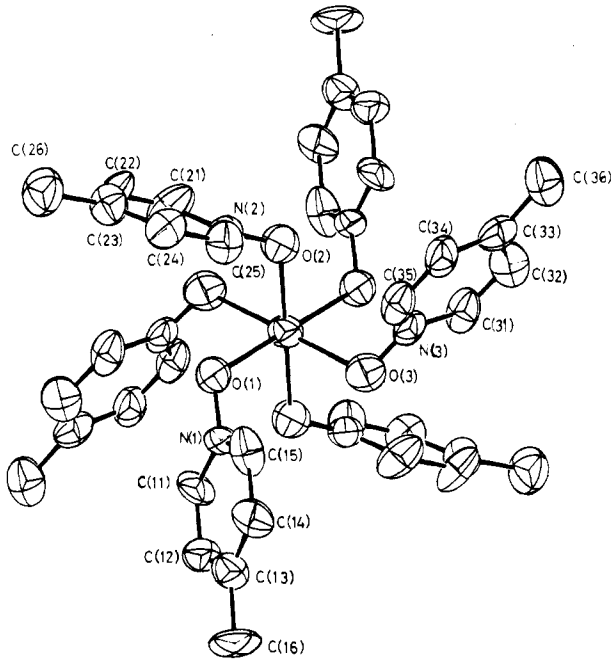

Figure 2. Perspective view of the $Zn(CH_3C_5H_4NO)_6^{2+}$ ion along the pseudo-threefold inversion axis of the cation. The atoms are labeled as in Table I.

netically inequivalent sites were resolved. Representative spectra are given in Figure 1. The **g** and (for the doped crystal) hyperfine splitting tensor data for both sites were obtained from the rotation data by a least-squares procedure using the program GAPLSD.[15] The average deviations at the least-squares minima were 0.002 and 0.005 in units of **g** for the pure and doped crystal data, respectively. Study of the variation of the spectra over the temperature range from 4.2 to 440 K for both pure and doped crystals showed no significant changes from those observed at room temperature. For pure crystals, there appears to be a first-order phase change at approximately 100–110 K. However, this results in only a small change in the principal values of the **g** tensors for the two sites. They become larger by about 0.015 upon lowering the temperature. No other changes were evident.

Results and Discussion

1. Structural Results. Pertinent structural data for the two complexes are given in Tables II and III while Figure 2 illustrates the configuration of the zinc complex cation viewed approximately along the [112] direction of the unit cell. Although the copper and zinc complexes are isomorphous and essentially isostructural, and the geometries of the MO_6 moieties in both depart significantly from O_h symmetry, there are in addition appreciable differences between the Cu–O and Zn–O bond distances which are attributable to the presence

Table III. Bond Distances (Å) and Best Plane Parameters for Picoline *N*-Oxide Ligands and Perchlorate Ions

	M = Cu	M = Zn
O(1)-N(1)	1.326 (11)	1.352 (9)
N(1)-C(11)	1.330 (15)	1.332 (12)
C(11)-C(12)	1.427 (19)	1.396 (14)
C(12)-C(13)	1.390 (19)	1.379 (15)
C(13)-C(14)	1.397 (19)	1.397 (15)
C(14)-C(15)	1.342 (19)	1.413 (15)
C(15)-N(1)	1.375 (16)	1.367 (13)
C(13)-C(16)	1.566 (19)	1.521 (15)
O(2)-N(2)	1.312 (12)	1.309 (9)
N(2)-C(21)	1.347 (17)	1.360 (13)
C(21)-C(22)	1.399 (20)	1.411 (15)
C(22)-C(23)	1.382 (18)	1.361 (15)
C(23)-C(24)	1.410 (19)	1.388 (15)
C(24)-C(25)	1.379 (20)	1.378 (16)
C(25)-N(2)	1.329 (17)	1.356 (13)
C(23)-C(26)	1.557 (18)	1.556 (15)
O(3)-N(3)	1.326 (14)	1.344 (10)
N(3)-C(31)	1.354 (17)	1.359 (12)
C(31)-C(32)	1.389 (22)	1.392 (16)
C(32)-C(33)	1.390 (21)	1.422 (16)
C(33)-C(34)	1.418 (21)	1.402 (15)
C(34)-C(35)	1.372 (20)	1.368 (15)
C(35)-N(5)	1.364 (17)	1.372 (13)
C(33)-C(36)	1.574 (22)	1.497 (16)
Cl-O(4)	1.347 (11)	1.373 (8)
Cl-O(5)	1.223 (22)	1.306 (13)
Cl-O(6)	1.318 (14)	1.356 (13)
Cl-O(7)	1.264 (21)	1.293 (16)

plane[a]	atoms	*l*	*m*	*n*	*d*
1	N(1)···C(15)	0.4604	−0.6186	−0.6367	8.36
2		0.5121	−0.6349	−0.5785	7.78
3	N(2)···C(25)	0.1137	−0.7265	0.6777	1.36
4		0.1792	−0.6894	0.7018	1.68
5	N(3)···C(35)	0.8109	0.4089	−0.4186	4.33
6		0.7812	0.4382	−0.4447	4.22

	dev[b]					
plane	N(*i*)	C(*i*1)	C(*i*2)	C(*i*3)	C(*i*4)	C(*i*5)
1	9	13	14	14	17	15
2	7	11	11	11	12	11
3	10	15	16	13	18	16
4	8	12	12	11	14	14
5	11	15	16	13	13	14
6	7	11	12	10	11	10

[a] The planes are defined as $lX + mY + nZ = d$ where *X*, *Y*, *Z* is an orthogonal system with *Y* and *Z* coincident with the *b* and *c* directions, respectively. For each pair of planes, the parameters for the copper complex are listed first. [b] Distances of atoms from planes (Å × 10^3).

of a Jahn–Teller distortion in the copper complex. Assuming that the bond distance variation in the zinc complex arises from the low site symmetry and that the same variation also applies to the copper complex, we calculate a value for the Jahn–Teller radius, R_{JT}, defined as

$$[\sum_{i=1}^{6}(\Delta d_{i(Cu)} - \Delta d_{i(Zn)})^2]^{1/2}$$

where $\Delta d_{i(M)}$ are the deviations of the individual M–O distances from their average,[16] of 0.39 Å. This agrees well with our previously reported value of 0.40 Å which was deduced from comparison of the thermal motion parameters for the pyridine *N*-oxide complexes $M(pyO)_6^{2+}$ of copper and zinc having S_6 symmetry.[2] This value led to predicted Cu–O bond lengths of 1.98 and 2.32 Å for the dynamically distorted complex.

The structure of the $M(CH_3C_4H_5NO)_6^{2+}$ ion depicted in Figure 2 indicates that the picoline *N*-oxide ligands coordinate to the metal to give approximate $\bar{3}$ (S_6) symmetry, this symmetry being found exactly for the rhombohedral $M(pyO)_6^{2+}$

(15) Keijzers, C. P.; Paulussen, G. F. M.; de Boer, E. *Mol. Phys.* **1975**, *29*, 1973.
(16) Ammeter, J. H.; Bürgi, H. B.; Gamp, E.; Meyer-Sandrin, V.; Jensen, W. P. *Inorg. Chem.* **1979**, *18*, 733.

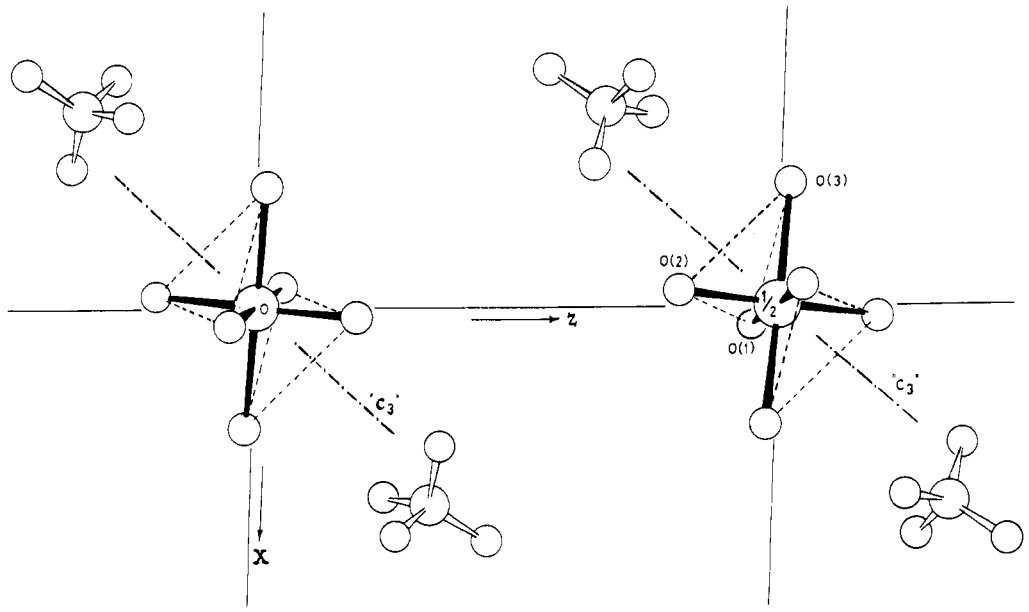

Figure 3. Projection of the structure of $Cu(CH_3C_5H_4NO)_6(ClO_4)$ onto (010) showing the relative orientations of the cation octahedra and the perchlorate ions.

complexes.[4,17] The inclinations of the ligand planes to the pseudothreefold axis vary from 6.3 to 23.2° in the two complexes, the value for this angle being 6.7° in the $Co(pyO)_6^{2+}$ complex.[17] It is this resulting nonlinear M–O–N ligand arrangement with the metal atom displaced appreciably from the planes of the pyridine rings that leads to the large deviations from octahedral electronic symmetry and the interesting magnetic ordering phenomena observed for the pyridine *N*-oxide complexes at low temperatures.

The packing of the complex cations and the perchlorate ions is illustrated in Figure 3, and this shows that the latter adopt the same orientation with respect to the cations that is found for the $M(pyO)_6^{2+}$ species, the anions in these structures being located on the crystal threefold axes. The monoclinic unit cells of the picoline *N*-oxide complexes can be viewed as the fusion of two mirror-related idealized rhombohedral unit cells (the *c* axis being approximately twice the length of the *a* and *b* axes) displaced relative to each other by half a lattice translation in the *a* direction. The pseudo-threefold axes (the [111] directions for the idealized unit cells) then lie approximately along the [112] and [$\bar{1}\bar{1}$2] direction in the monoclinic cell, and for the copper complex, the directions of the long Cu–O bonds are mutually inclined at an angle of 19.7° so that the arrangement of complex cations can be described as being approximately ferrodistortive. It is clear from both the EPR and X-ray measurements that the picoline *N*-oxide complex is very similar to the monoclinic form of the nitrate complex $Cu(C_5H_5NO)_6(NO_3)_2$ described earlier,[2,9] which cocrystallizes with the rhombohedral form from ethanolic solution. The geometries of the picoline *N*-oxide ligands in both complexes appear to be normal, the bond angles varying from 123.3 to 116.1°. As noted earlier, the perchlorate ions are undergoing very extensive librational motion, and for these, the bond angles range from 92.8 to 118.4°.

2. EPR Results. Table IV lists the principal EPR parameters for the two magnetically inequivalent sites in the pure and doped crystals of the picoline *N*-oxide complexes, and it can be seen from these that the **g** tensors are in accord with a tetragonally elongated geometry for the copper ion coordination sphere, the sequence $g_3 > g_2 \approx g_1 > g_e$ being that expected for an $|x^2 - y^2\rangle$ ground state. There is, however, an appreciable rhombic component to the **g** tensors for both the pure and doped crystals which can probably be attributed principally to the significant deviation of the coordination sphere from D_{4h} geometry. This component is significantly larger than that found for the low-temperature sites of the pure and doped pyridine *N*-oxide complexes.[2,3]

As noted in the introductory section there is no significant temperature variation of the EPR spectrum for either the doped or the pure crystals, indicating that the Jahn–Teller effect is static, only one site being significantly populated. The similarity between the principal values of the **g** tensors given in Table IV shows that presumably there is sufficient flexibility

Table IV. Single-Crystal EPR Parameters for $Cu(CH_3C_5H_4NO)_6(ClO_4)_2$

(a) Pure Complex

site 1				site 2			
$g_1 = 2.067$				$g_1 = 2.067$			
$g_2 = 2.123$				$g_2 = 2.124$			
$g_3 = 2.316$				$g_3 = 2.316$			
orientation 1[a]				orientation 2			
	x	y	z		x	y	z
g_1	4.2°	93.5	98.9	g_1	3.6°	98.9	98.3
g_2	86.6°	6.5°	96.9°	g_2	89.9	5.9°	97.2
g_3	92.5°	84.6°	10.5°	g_3	93.6	84.2°	7.3

(b) Doped Complex

site 1				site 2			
$g_1 = 2.068$				$g_1 = 2.077$			
$g_2 = 2.112$				$g_2 = 2.111$			
$g_3 = 2.325$				$g_3 = 2.321$			
$A_1 = 0.0$				$A_1 = 0.0$			
$A_2 = 26.4 \times 10^{-4}$ cm^{-1}				$A_2 = 27.5 \times 10^{-4}$ cm^{-1}			
$A_3 = 119.5 \times 10^{-4}$ cm^{-1}				$A_3 = 118.7 \times 10^{-4}$ cm^{-1}			
orientation 1				orientation 2			
	x	y	z		x	y	z
g_1	18.5°	108.7	98.9	g_1	14.4	103.6	87.0
g_2	71.5	20.5°	100.0	g_2	79.9	16.5	104.0
g_3	90.4	88.7	9.9°	g_3	93.3°	80.8	13.2

[a] The axes x, y, z correspond to the metal-oxygen bond vectors, along M–O(1), M–O(2), and M–O(3), respectively, with the positive octant containing the pseudo-threefold axis of the cation.

(17) Bergendahl, T. J.; Wood, J. S. *Inorg. Chem.* **1975**, *14*, 338. Taylor, D. *Aust. J. Chem.* **1978**, *31*, 713.

in the host lattice to allow the copper ion to take up the same specific tetragonally elongated symmetry as in the pure crystal, and, therefore, a dynamic Jahn–Teller effect is not observed. From the differing orientations of the **g** tensors in the doped and pure crystals, it can be inferred that together with the tetragonal distortion a rotation of about 10° takes place around the elongated axis. The orientation angle data for the pure complex shows that the axes of the **g** tensor are not coincident with the copper–oxygen bond directions. This was also found to be the case for the pyridine *N*-oxide complexes, and as for these species the principal axis of the **g** tensor (assuming it to be basically axial) is directed into the region of the ligand N–O bond. This is in agreement with the now well-established result that this group of complexes deviate markedly from octahedral symmetry with regard to their electronic properties.[18]

As a final point we note that there is no significant spin exchange between the two magnetically inequivalent sites in the pure complex. This can be seen qualitatively, in that the **g** tensors for the sites in the pure and doped crystals agree well with one another, and quantitatively from simulation of the ESR spectra, taking into account exchange interaction with the help of the modified Bloch equations. These calculations show the exchange constant to be very small. In fact, the exchange must be in the order of the copper hyperfine splitting since the latter cannot be observed in the pure system. The line width is, however, still determined by the hyperfine splitting and is maximal in the direction of the maximum g value where also the largest hyperfine splitting is expected. The line shape is in between Lorentzian and Gaussian, proving again that the exchange is small. In the case of the monoclinic phase of the pyridine *N*-oxide nitrate complex, the exchange is also small, as a consequence (at Q-band frequency) two lines are observed.[19] This is in contrast to the pure trigonal pyridine *N*-oxide complexes where the exchange interaction is much larger and amounts to about 0.7 cm^{-1}. The relevant copper–copper distances are 9.45 and 10.55 Å for the trigonal and monoclinic pyridine *N*-oxide complexes and 11.57 Å for the picoline *N*-oxide complex.

Acknowledgment. We thank the Scientific Affairs Division of NATO for support of this research through Grant No. 1432. A.E.Y. acknowledges the receipt of a research fellowship (1979–1980) from the Faculty of Science, University of Nijmegen, The Netherlands.

Registry No. $Cu(CH_3C_5H_4NO)_6(ClO_4)_2$, 35828-27-4; $Zn(CH_3C_5H_4NO)_6(ClO_4)_2$, 24470-65-3.

Supplementary Material Available: Anisotropic thermal parameter and structure factor tables for Cu- and $Zn(CH_3C_5H_4NO)_6(ClO_4)_2$ (8 pages). Ordering information is given on any current masthead page.

(18) Mackay, D. J.; Evans, S. V.; McMeeking, R. F. *J. Chem. Soc., Dalton Trans.* **1978**, 160.

(19) Keijzers, C. P.; Wood, J. S., unpublished work.

Contribution from the Department of Plastics Research and of Structural Chemistry, The Weizmann Institute of Science, Rehovot, Israel

Synthesis and Properties of Tetraphenylporphyrin Molecules Containing Heteroatoms Other Than Nitrogen. 6. Electrochemical Studies

ABRAHAM ULMAN,*[1] JOOST MANASSEN, FELIX FROLOW, and DOV RABINOVICH

Received March 18, 1980

When the two NH groups in tetraphenylporphyrin (TPP) are replaced by the group 6A heteroatoms S, Se, and Te, bonding interactions within the porphinato core are formed as is apparent from their short distances as found in X-ray structure analysis and is also supported by MO calculations. Because of the heterosubstitution there is a change in the energies of the frontier orbitals in such a way that the LUMO is stabilized. The HOMO is stabilized because the short distances between the chalcogen atoms give rise to the formation of $d\pi$–$d\pi$ orbitals, which interact with the frontier orbitals. These stabilization mechanisms are expressed by positive shifts of both the reduction and the oxidation potentials as measured by cyclic voltammetry. It appears that there is a linear relationship between the difference between the first oxidation and first reduction potential (which decreases with the increasing bonding interaction) and $1/\lambda_{max}$ (cm^{-1}) of the Soret transition. The decrease of the first reduction potential relates linearily to the chemical shifts of the β-hydrogens in the ^{1}HMR spectra. For the para-substituted S_2TPP molecules the Hammett constant ρ for the first oxidation reaction is abnormally large. This is connected with the nonplanarily of the cation radicals. The optical spectrum of the Se_2TPP cation radical provides support for this suggestion.

Introduction

Electrochemistry as a tool for the study of the physical properties of porphyrins and metalloporphyrins has been extensively used recently.[2] The influence of the metal ion, the axial ligand, and the para substituents on the half-wave potentials is well established.[3-18]

The effect of substituents on the oxidation and reduction reactions of the π system of tetraphenylporphyrin (TPP) was investigated by Kadish et al. by cyclic voltammetry in methylene chloride[18] and in other solvents.[14] In all solvents it was found that electron-donating substituents shift the oxidation and the reduction potentials to more positive values. Elec-

(1) To whom correspondence should be addressed at the Department of Organic Chemistry, Makhteshim Chemical Works Ltd., P.O. Box 60, Beer-Sheva 84100, Israel.
(2) Smith, K. M. "Porphyrins and Metalloporphyrins"; Elsevier: New York, 1975; Chapter 14.
(3) Fuherhop, J.-H.; et al. *J. Am. Chem. Soc.* **1973**, *95*, 5140–5147.
(4) Wolberg, A.; Manassen, J. *J. Am. Chem. Soc.* **1970**, *92*, 2982.
(5) Walker, F. A.; et al. *J. Am. Chem. Soc.* **1975**, *97*, 2390–2397.
(6) Felton, R. H.; Linschitz, H. *J. Am. Chem. Soc.* **1966**, *88*, 1113–1116.
(7) Clark, D. W.; Hush, N. S. *J. Am. Chem. Soc.* **1965**, *87*, 4238–4242.
(8) Fajer, J.; et al. *J. Am. Chem. Soc.* **1970**, *92*, 3451–3459.
(9) Dolphin, D.; Felton, R. H. *Acc. Chem. Res.* **1974**, *7*, 26–32.
(10) Kadish, K. M.; et al. *Angew. Chem., Int. Ed. Engl.* **1972**, *11*, 1014–1016.
(11) Felton, R. H.; et al. *J. Am. Chem. Soc.* **1971**, *93*, 6332–6334.
(12) Kadish, K. M.; et al. *J. Am. Chem. Soc.* **1974**, *96*, 591, 592.
(13) Kadish, K. M.; et al. *J. Am. Chem. Soc.* **1975**, *97*, 282–288.
(14) Kadish, K. M.; Morrison, M. M. *J. Am. Chem. Soc.* **1976**, *98*, 3326–3328.
(15) Kadish, K. M.; Morrison, M. M. *Inorg. Chem.* **1976**, *15*, 980–982.
(16) Walker, F. A.; et al. *J. Am. Chem. Soc.* **1976**, *98*, 3484–3489.
(17) Kadish, K. M.; Larson, C. *Bioinorg. Chem.* **1977**, *7*, 95–105.
(18) Kadish, K. M.; Morrison, M. M. *Bioinorg. Chem.* **1977**, *7*, 107–115.

0020-1669/81/1320-1987$01.25/0